

States in  $O^{16}$  between 12.67 and 13.80 Mev\*

F. B. HAGEDORN†

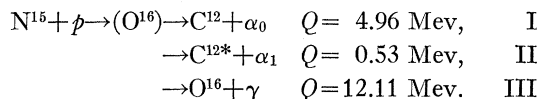
*Kellogg Radiation Laboratory, California Institute of Technology, Pasadena, California*

(Received July 8, 1957)

A study of the elastic scattering of protons from  $N^{15}$  is reported for proton energies between 600 and 1800 kev and for scattering angles from  $75^\circ$  to  $160^\circ$ . The technique for the preparation of the  $N^{15}$  targets is discussed. Anomalies in the scattering cross section are observed near incident proton energies of 710, 898, 1028, 1210, and 1640 kev, corresponding to states in  $O^{16}$  from 12.78 to 13.65 Mev. Analysis of these scattering data leads to the assignments  $J=0^-$ ,  $J=2^-$ ,  $J=1^-$ ,  $J=3^-$ , and  $J=1^+$  for the 710, 898, 1028, 1210, and 1640-kev states respectively. These assignments agree with earlier work except for the 710-kev resonance, which is reported here for the first time, and the 1210-kev level, which was previously reported to be  $J=4^+$ . The angular distribution of the  $\alpha$ -particles resonant at 1210 kev from the reaction  $N^{15}(p,\alpha\gamma)C^{12}$  has been remeasured and requires  $J=4^+$  as was found previously. However, a measurement of the  $\alpha$ - $\gamma$  angular correlation function at 1210 kev is found to be consistent with  $J=3^-$  but not  $J=4^+$ . This discrepancy has not been resolved, but the evidence favoring the assignment  $J=3^-$  is quite strong. Suggestions for the isotopic spin quantum numbers for these five states in  $O^{16}$  are made.

## I. INTRODUCTION

THE region of excitation in the  $O^{16}$  nucleus above 12.11 Mev has been studied in some considerable detail<sup>1-10</sup> by means of reactions induced by bombarding  $N^{15}$  with protons. These reactions, for incident protons with energies less than about 2.9 Mev, are:



Resonances have been reported for reaction I, for incident protons with energies less than 1800 kev, near 340 kev ( $J=0^+$  or  $1^-$ ), 1050 kev ( $J=1^-$ ), and 1210 kev ( $J=4^+$ ) and for reaction II near 429 kev ( $J=2^-$ ), 898 kev ( $J=2^-$ ), 1050 kev ( $J=1^-$ ), 1210 kev ( $J=4^+$ ), and 1640 kev ( $J=1^+$  or  $2^-$ ). A single resonance, near 1050 kev, has been reported for capture radiation to the ground state of  $O^{16}$  (reaction III). Schematic excitation functions for these three reactions may be seen in Fig. 1.

Since there has been some ambiguity in the assignments for certain of these states in  $O^{16}$ , it has seemed useful to study the same region of excitation through a different process, proton elastic scattering. In addition to permitting a clear assignment of spin and parity in many otherwise obscure cases, this technique often permits the determination of important nuclear

parameters not obtainable by other methods. Sometimes, as was the case in the present work, elastic scattering reveals resonances not detected by other means.

A preliminary report of this work has been presented at a meeting of the American Physical Society,<sup>11</sup> and a similar study has been reported under way by the Iowa group.<sup>12</sup>

## II. EXPERIMENTAL PROCEDURE

The apparatus used in this investigation has been described in earlier publications from this laboratory. A well-defined proton beam is produced in a 2-Mv electrostatic accelerator and deflected through 80 degrees in an electrostatic analyzer. The stability and control of the system is such that the beam is homogeneous in energy to 0.05–0.1%. Protons elastically scattered from a suitably placed target are analyzed in a 180-degree double-focusing magnetic spectrometer,<sup>13</sup> so mounted as to permit continuously variable angular settings from  $0^\circ$  to  $160^\circ$  in the laboratory system. The scattered protons are detected with a

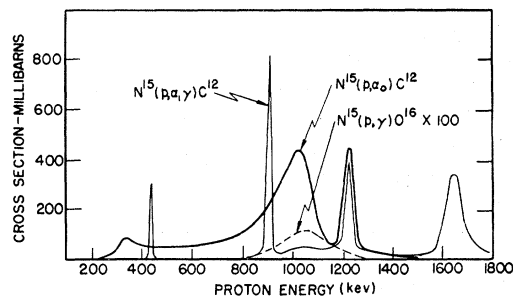


FIG. 1. Schematic excitation functions for  $N^{15} + p$  reactions. The widths of the narrow resonances are not drawn to scale.

\* Supported in part by the joint program of the Office of Naval Research and the U. S. Atomic Energy Commission.

† Now at Bell Telephone Laboratories, Murray Hill, New Jersey.

<sup>1</sup> Barnes, James, and Neilson, *Can. J. Phys.* **30**, 717 (1952).

<sup>2</sup> Schardt, Fowler, and Lauritsen, *Phys. Rev.* **86**, 527 (1952).

<sup>3</sup> J. Seed and A. P. French, *Phil. Mag.* **43**, 1214 (1952).

<sup>4</sup> A. V. Cohen and A. P. French, *Phil. Mag.* **44**, 1259 (1953).

<sup>5</sup> Kraus, French, Fowler, and Lauritsen, *Phys. Rev.* **89**, 299 (1953).

<sup>6</sup> Neilson, James, and Barnes, *Phys. Rev.* **92**, 1084(A) (1953).

<sup>7</sup> A. A. Kraus, Jr., *Phys. Rev.* **94**, 975 (1954).

<sup>8</sup> S. Bashkin and R. R. Carlson, *Phys. Rev.* **106**, 261 (1957).

<sup>9</sup> Jacobs, Bashkin, and Carlson, *Bull. Am. Phys. Soc. Ser. II*, **1**, 212 (1956).

<sup>10</sup> Lidofsky, Jones, Bent, Weil, Kruse, Bardon, and Havens, *Bull. Am. Phys. Soc. Ser. II*, **1**, 212 (1956).

<sup>11</sup> F. B. Hagedorn, *Bull. Am. Phys. Soc. Ser. II*, **1**, 387 (1956).

<sup>12</sup> Bashkin, Carlson, and Jacobs, *Bull. Am. Phys. Soc. Ser. II*, **1**, 212 (1956).

<sup>13</sup> Snyder, Rubin, Fowler, and Luaritsen, *Rev. Sci. Instr.* **21**, 852 (1950).

cesium iodide crystal 0.005 in. thick, placed at the exit slit of the spectrometer. For the angular correlation experiment, a low-resolution, alternating-gradient magnetic spectrometer<sup>14</sup> selected the  $\alpha$  particles, and a  $1\frac{1}{2}$  in.  $\times$   $1\frac{3}{4}$  in. sodium iodide crystal detected the 4.43-Mev gamma radiation.

Preparation of a suitable target is often the most difficult technical problem in work of this kind. Since the momentum of an elastically scattered proton depends on the mass of the scattering nucleus, selecting an interval of momenta with the magnetic spectrometer allows one in principle to discriminate against protons scattered from nuclei of mass different from the one under observation. Two important restrictions on the target composition are necessary in order to make this discrimination practical, however. Because the magnetic spectrometer does not have ideal resolving characteristics, nuclei of mass numbers adjacent to the proposed target nucleus should preferably not be present in the target. In addition, all nuclei heavier than the proposed target nucleus are objectionable in a thick target. Since protons which penetrate beneath the surface of a thick target or thick backing lose varying amounts of energy in the process, a proton scattered from a heavy nucleus somewhere beneath the surface can emerge from the target with the same momentum and direction as does a proton scattered from a light nucleus in the target surface. The background so produced is ordinarily at least as large as the effect under observation and makes precise measurements quite impracticable. The combination of requirements of low contamination, light element backing, and target stability poses an exceptionally difficult problem in the case of  $N^{15}$ .

Most of the targets used in the present work were prepared in a small isotope separator constructed for the purpose. A radio-frequency ion source was supplied with nitrogen gas produced from  $NH_4NO_3$  in which 65% of the  $NH_4$  radicals contained  $N^{15}$ . The resulting ions were accelerated to about 20 keV, focused, and magnetically analyzed. It was found that about 90% of the nitrogen beam consisted of the molecular ions  $N^{14}N^{14}$ ,  $N^{14}N^{15}$ , and  $N^{15}N^{15}$ ; the last-mentioned amounted to about 6 microamperes in a spot  $\frac{1}{8}$  in. by  $\frac{1}{4}$  in. Dilution with 20 parts of purified helium to one part of the nitrogen supplied to the ion source reduced the nitrogen ion output by less than 30% and considerably reduced the consumption of enriched gas. Separation of the mass 29 and mass 30 beams in the analyzing magnet was sufficiently great so that negligible  $N^{14}$  contamination resulted from the mass 29 beam. Such contamination as did occur is attributed to the presence in small quantities of the ion  $(N^{14})_2(H^1)_2$  and to the absorption of residual  $N^{14}$  and  $O^{16}$  from the vacuum system.

Graphite was found to be the most satisfactory material in which to collect the  $N^{15}$ . Such targets proved

to be quite stable under proton bombardment up to  $0.5 \mu a$  per square millimeter and could safely be heated to  $400^\circ C$ . Saturation was found to occur at an areal density of about  $1.5 \times 10^{17}$  nitrogen atoms per square centimeter, corresponding approximately to one nitrogen atom per four carbon atoms. It is presumed that chemical binding of the nitrogen to the carbon occurs. Momentum profiles of protons elastically scattered through three different angles from an  $N^{15}$  target in graphite are shown in Fig. 2.  $N^{15}$  atoms are about 8 times more numerous than  $O^{16}$  atoms and about 15 times more numerous than  $N^{14}$  atoms in this target.

In principle, momentum profiles such as those of Fig. 2 are obtained for each angle and each bombarding energy. The elastic scattering cross section is then calculated from the area under the  $N^{15}$  peak, the spectrometer resolution and solid angle, the number of protons incident on the target, and the number of  $N^{15}$  atoms per unit area in the target. For scattering angles smaller than  $120^\circ$ , the  $N^{14}$  and  $O^{16}$  peaks are incompletely resolved in the present work, and it is necessary to subtract their contributions from the total area. Measuring the areas at  $160^\circ$ , where the peaks are well separated, permitted calculation of the contributions at other angles, using the known<sup>15-17</sup> scattering cross sections for  $N^{14}$  and  $O^{16}$ .

The number of  $N^{15}$  atoms per unit area in the elastic scattering targets prepared in the isotope separator was determined by comparing the thin-target yield of the 4.43-Mev gamma rays (reaction II) integrated over the 898-keV resonance, with the yield from a semithick  $N^{15}$  target of known composition. For a thin target and an isolated narrow resonance, the integrated

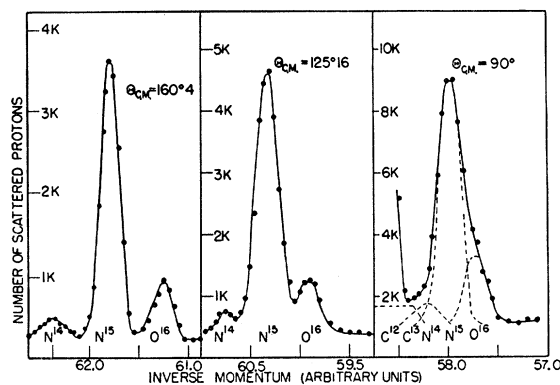


FIG. 2. Momentum profiles of protons elastically scattered from  $N^{15}$  embedded in graphite. The scattering angles were  $160^\circ 4'$ ,  $125^\circ 16'$ , and  $90^\circ$ , and the incident proton energy was 1300 keV. The dashed lines on the  $90^\circ$ -profile indicate approximately the contributions from  $O^{16}$ ,  $N^{15}$ ,  $N^{14}$ , and  $C^{12}$ .

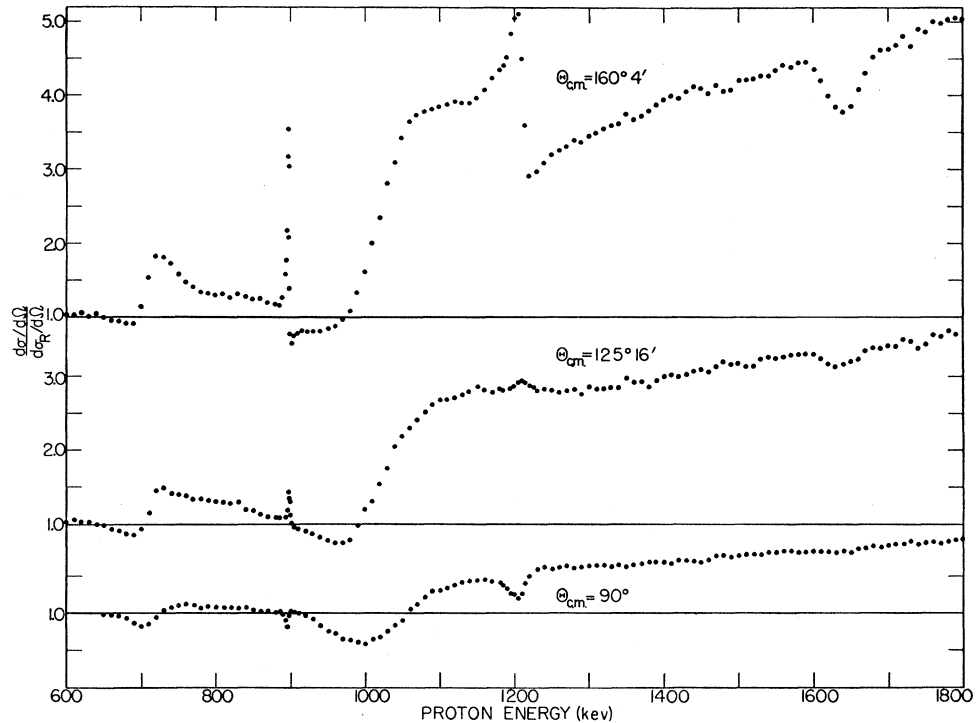
<sup>15</sup> Hagedorn, Mozer, Webb, Fowler, and Lauritsen, Phys. Rev. **105**, 219 (1957).

<sup>16</sup> Laubenstein, Laubenstein, Koester, and Mobley, Phys. Rev. **84**, 12 (1951).

<sup>17</sup> Eppling, Cameron, Davis, Divatia, Galonsky, Goldberg, and Hill, Phys. Rev. **91**, 438(A) (1953).

<sup>14</sup> H. J. Martin and A. A. Kraus, Rev. Sci. Instr. **28**, 175 (1957).

FIG. 3. Ratios of the observed N<sup>15</sup>(*pp*)N<sup>15</sup> differential cross sections to the Rutherford cross sections for scattering angles of 160°4', 125°16', and 90° and for incident proton energies between 600 and 1800 kev.



yield per incident proton is given by

$$\int_0^{\infty} Y_{\text{thin}}(E) dE = \pi \sigma_R \Gamma n_T / 2,$$

where  $\sigma_R$  is the resonant cross section,  $\Gamma$  is the full width of the resonance at half-maximum, and  $n_T$  is the number of N<sup>15</sup> atoms per unit area in the target. For an infinitely thick target, the maximum yield per incident proton is given by

$$Y_{\text{thick}} = \pi \sigma_R \Gamma / 2\epsilon,$$

where  $\epsilon$  is the stopping cross section for protons per N<sup>15</sup> atom in the thick target material. A comparison of the two above expressions results in

$$n_T = \int_0^{\infty} Y_{\text{thin}}(E) dE / (\epsilon Y_{\text{thick}}).$$

The thick-target yield was obtained with a 50-kev evaporated layer of KNO<sub>3</sub> enriched to 61% in N<sup>15</sup>; since the resonance has an intrinsic width of only 2.2 kev, extrapolation to infinite thickness introduced a negligible uncertainty. The stopping cross section  $\epsilon$  for protons in KNO<sub>3</sub> was obtained by adding the atomic stopping cross sections of potassium, nitrogen, and oxygen. Values for nitrogen and oxygen were taken from the compilation of Fuchs and Whaling,<sup>18</sup> and the potassium value was obtained by interpolation of a plot

<sup>18</sup> R. Fuchs and W. Whaling (unpublished).

of measured stopping cross sections against atomic number. The resulting value for  $\epsilon(\text{KNO}_3)$  is  $5.57 \times 10^{-14}$  ev cm<sup>2</sup> per N<sup>15</sup> nucleus, with an uncertainty of about 6%. An additional uncertainty of 5 or 6% is involved in the experimental measurement of the ratio of yields from the thick and thin targets, resulting in an over-all probable error of about 8% in  $n_T$ .

The normalization of the scattering cross section was carried out at an incident proton energy of 1100 kev and at a center-of-mass scattering angle of 160°4'. At this energy and angle, the differential cross section was found to be  $219 \pm 24$  millibarns per steradian. The probable error for the absolute value of the elastic scattering cross section is about 11%, the major source of which is in the evaluation of  $n_T$ . Other contributing factors are uncertainties in measuring the areas under the N<sup>15</sup> peaks, and in the calibrations of the current integrator, electrostatic analyzer, and magnetic spectrometer. Relative cross sections have been assigned probable errors dependent on the difference in energy and angle between the two points under consideration. A 2% error is estimated for relative values at the same angle and for energy differences not greater than 50 kev. This estimate rises to 12% for large differences in energy and angle.

The proton energy range for which measurements have been made extends from 600 to 1800 kev. The upper limit is that of the available proton beam, while the lower limit is imposed by the nature of the targets. Near 600 kev, at a scattering angle of 90°, almost half of the N<sup>15</sup> peak is masked by the thick-target C<sup>12</sup> step.

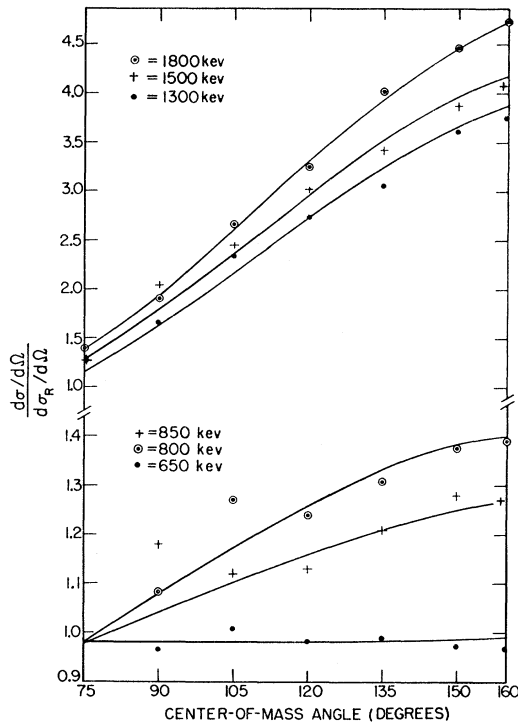


FIG. 4. Angular distributions at incident proton energies corresponding to nonresonant regions of the excitation functions. The curves have been calculated by using the nonresonant phase shifts given in the text.

The data of Fig. 2 indicate the beginning of this masking at  $90^\circ$  even at 1300-keV incident proton energy.

### III. EXPERIMENTAL RESULTS AND ANALYSIS

The elastic scattering data are presented as ratios of the measured differential cross sections to the Rutherford cross sections. The observed energy dependence of these ratios for three scattering angles is shown in Fig. 3 for the entire range of incident proton energies used in the present work. Pronounced anomalies are observed near 710, 898, 1028, 1210, and 1640 keV. All of these anomalies except the first correspond to previously reported states in  $O^{16}$ . In addition to the data of Fig. 3, detailed angular distributions were obtained at selected energies both near to and between the anomalies.

The general expression for the scattering cross section and the detailed techniques of analysis have been discussed fully by Christy<sup>19</sup> and by Mozer.<sup>20</sup> The parameters of interest here are the orbital angular momentum  $l$ , the total angular momentum  $J$ , the channel spin ratio  $\alpha$ , the ratio of the partial proton width to the total width  $\Gamma_p/\Gamma$ , and the resonant and nonresonant nuclear phase shifts. With scattering data of limited accuracy, it is not possible to evaluate each of these parameters uniquely. How-

ever, considerable information is available from the reaction data, and full use of this information has been made in the present analysis.

As a first step, the nonresonant phase shifts (potential phase shifts) were evaluated from a series of angular distributions taken at energies away from resonances. A selection of these angular distributions is shown in Fig. 4, where the ratios of the observed to Rutherford cross sections are plotted as a function of scattering angle. It was found that these distributions could be fitted well within the accuracy of the observations by the assumption of only  $s$ -wave nonresonant scattering, the resulting two phase shifts being about equal and varying nearly linearly with energy from  $-4^\circ$  at 650 keV to  $-22^\circ$  at 1800 keV. The solid lines in Fig. 4 have been calculated using these assumptions, taking into account small contributions due to the resonant scattering from the broad levels. In the analysis of the regions containing the anomalies, a smooth interpolation of the nonresonant phase shifts was assumed. This analysis will be treated in detail for each state in the following paragraphs.

$E_p=710$  keV.—The state near 710 keV did not appear in earlier studies of reactions I, II, or III. After it was observed in the present work, a search was made for possible cascading capture radiation. A weak radiation was found, exhibiting resonance near 710 keV. An excitation function of this radiation is shown in Fig. 5, together with a calculated curve based on the Breit-Wigner single level formula with the parameters  $E_R=710\pm 7$  keV and  $\Gamma(E_R)=40\pm 4$  keV. The target thickness (35-keV layer of enriched  $KNO_3$ ) and the energy variation of the penetration factor have been taken into account in this calculation. A pulse-height analysis of this resonant gamma radiation indicates quantum energies near 7.0 and 5.5 MeV, consistent with a cascade through the 6.9- or 7.1-MeV states in  $O^{16}$ .

The absence of  $\alpha$ -particle groups associated with this resonance indicates that  $\Gamma_p/\Gamma \approx 1$ . The observed width then corresponds to 0.1, 0.5, or 8.0 for the ratio of the reduced width to the single-particle limit,  $3\hbar^2/2MR^2$ , for  $s$ -,  $p$ -, or  $d$ -wave protons respectively. Interference

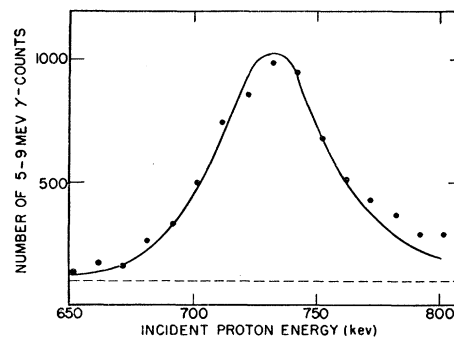


FIG. 5. Excitation function of capture radiation cascading from the  $E_p=710$ -keV resonance. The solid curve has been calculated for  $E_R=710$  keV and  $\Gamma(E_R)=40$  keV.

<sup>19</sup> R. F. Christy, *Physica* **22**, 1009 (1956).

<sup>20</sup> F. S. Mozer, *Phys. Rev.* **104**, 1386 (1956).

minima near 710 keV are observed in the elastic scattering data of Fig. 3 at roots of the first, second, and third Legendre polynomials and hence exclude  $p$ -,  $d$ -, or  $f$ -wave formation. It may be concluded that this state is formed by  $s$ -wave protons and therefore has  $J=0^-$  or  $1^-$ . For  $s$ -wave formation, the calculated magnitude of the anomaly,  $(d\sigma/d\sigma_R)_{\max} - (d\sigma/d\sigma_R)_{\min}$ , is 0.99 for the assignment  $J=0^-$  and 2.97 for  $J=1^-$ , at the  $160^\circ$  scattering angle. The observed anomaly size,  $0.94 \pm 0.10$ , clearly excludes the latter assignment. With the assumption  $J=0^-$ , angular distributions have been calculated for five energies near the resonance, and these distributions are compared with the experimental results in Fig. 6. The assignment  $J=0^-$  is also consistent with the nonappearance of this state in the studies of reactions I, II, and III.

$E_p=898$  keV.—Considerable information concerning the 898-keV state has been obtained previously from studies<sup>1,2,3,5</sup> of reaction II. This state has been shown to be formed by  $d$ -wave protons, and the assignment  $J=2^-$  has been deduced. Values of the resonant phase shift as a function of energy and of the channel spin ratio have also been determined. As may be seen in Fig. 3 and in more detail in Fig. 7, the anomaly in the scattering cross section associated with the 898-keV state is symmetric around the resonance energy at a scattering angle of  $125^\circ 16'$ . This vanishing of anti-symmetric terms at a root of the second Legendre polynomial independently establishes  $d$ -wave formation of the state. A state in O<sup>16</sup> formed by  $d$ -wave protons plus N<sup>15</sup> may have  $J=1^-, 2^-,$  or  $3^-$ . Excitation functions have been calculated for these three choices, using reaction data to evaluate all of the parameters in the

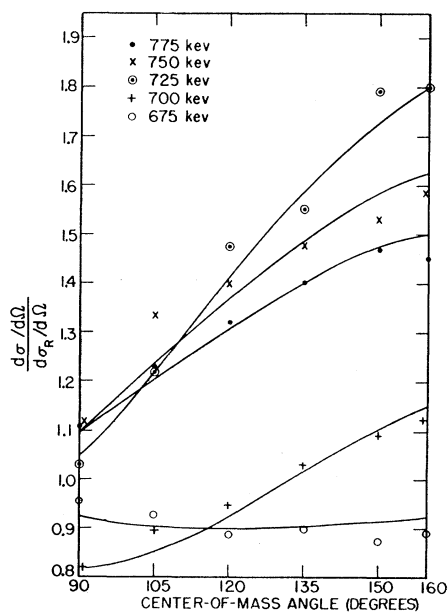


FIG. 6. Angular distributions at incident proton energies near the 710-keV resonance. The curves have been calculated for  $E_R=710$  keV,  $\Gamma(E_R)=40$  keV,  $\Gamma_p/\Gamma=1$ , and  $J=0^-$ .

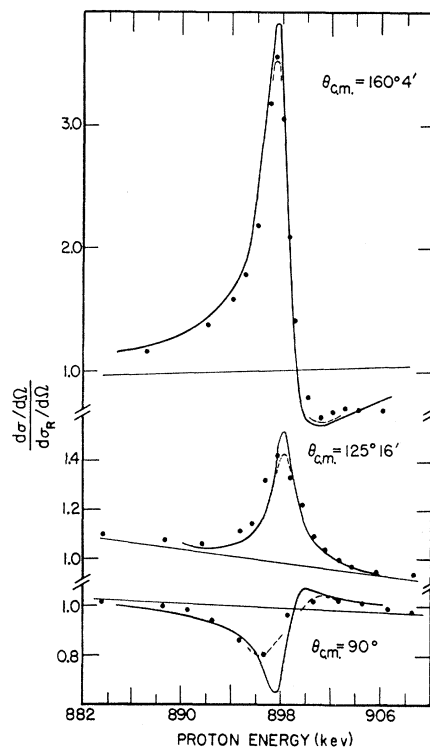


FIG. 7. Excitation functions of the elastic scattering near the 898-keV resonance. The solid curves have been calculated for  $E_R=898$  keV,  $\Gamma=2.2$  keV,  $\Gamma_p/\Gamma=0.56$  and  $J=2^-$ . The dashed lines indicate corrections for the finite resolution of the experiment.

cross-section expressions except  $\Gamma_p/\Gamma$ . Only the assignment  $J=2^-$  was found to be consistent with the present results, and  $\Gamma_p/\Gamma=0.56$  was obtained. The solid curves in Fig. 7 have been calculated using these assumptions, and the dashed lines take resolution effects into account.

With  $J$  and  $\Gamma_p/\Gamma$  known, the total reaction cross section may be calculated from the Breit-Wigner expression:  $\sigma_R=4\pi\omega\lambda^2\Gamma_p(1-\Gamma_p/\Gamma)/\Gamma$ . This calculation yields 1.02 barns, in satisfactory agreement with the measured value of  $0.83 \pm 0.20$  barn reported by Kraus *et al.*<sup>5</sup>

$E_p=1028$  keV.—The strong anomaly in the elastic scattering near 1000 keV (see Fig. 3) is presumably associated with the resonance for reactions I, II, and III reported earlier at  $E_p=1050$  keV. To locate the resonance more precisely and to determine its width, the thin target excitation function for capture radiation was measured, with the results shown in Fig. 8. A satisfactory fit to the data is obtained with a Breit-Wigner function with the parameters  $E_R=1028 \pm 10$  keV,  $\Gamma(E_R)=140 \pm 7$  keV. As is the case for the 710-keV resonance,  $s$ -wave formation is indicated both by the great width of the resonance and by the elastic scattering, and the magnitude of the anomaly requires  $J=1^-$ , with  $\Gamma_p/\Gamma=0.80$ . Calculated elastic scattering angular distributions based on these parameters are compared with the measured cross sections in Fig. 9.

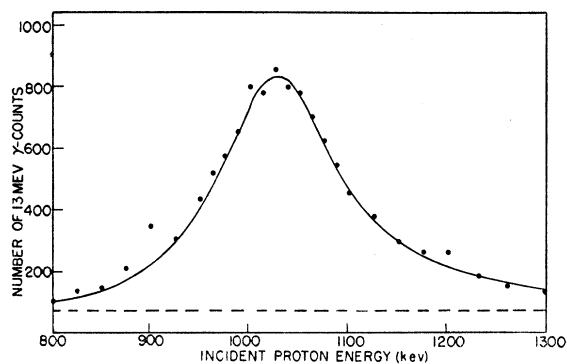


FIG. 8. Excitation functions of the capture radiation from the 1028-keV resonance. The solid curve has been calculated for  $E_R=1028$  keV and  $\Gamma(E_R)=140$  keV.

The agreement obtained is quite satisfactory and would appear to exclude the possibility of two states in this neighborhood. From the fact that both  $\alpha$  particles and electric dipole  $\gamma$  radiation are emitted, it may be concluded that the  $O^{16}$  state contains a mixture of  $T=0$  and  $T=1$  character.<sup>21</sup> The calculated reaction cross section is 0.35 barn, in good agreement with the measured value of 0.4 barn.<sup>2,22</sup> The assignment  $J=1^-$  has been suggested previously to account for the relatively large radiative width.<sup>2</sup>

$E_p=1640$  keV.—The analysis of the 1640-keV data, shown in detail in Fig. 10, is similar to that at 898 keV. Formation by  $p$ -wave protons is suggested by the absence of antisymmetric terms at  $90^\circ$ , allowing  $J=0^+$ ,

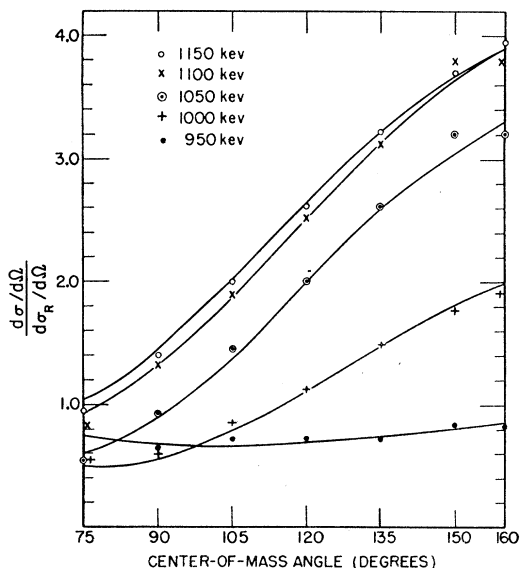


FIG. 9. Angular distributions at incident proton energies near the 1028-keV resonance. The curves have been calculated for  $E_R=1028$  keV,  $\Gamma(E_R)=140$  keV,  $\Gamma_p/\Gamma=0.80$ , and  $J=1^-$ .

<sup>21</sup> D. H. Wilkinson, Phys. Rev. **90**, 721 (1953).

<sup>22</sup> F. B. Hagedorn and J. B. Marion, Phys. Rev. (to be published).

$1^+$ , or  $2^+$ . Choosing a unique value of  $J$  on the basis of the scattering data alone is not possible in this case, however. Assuming  $p$ -wave formation, one can show that the anomaly size at  $90^\circ$  depends on  $J$  and  $\Gamma_p/\Gamma$  only in the factor  $(2J+1)(\Gamma_p/\Gamma)^2$ . The data indicate that this factor is much less than unity for this state. At other angles, the dependence on  $J$  and  $\Gamma_p/\Gamma$  lies in a term proportional to  $(2J+1)\Gamma_p/\Gamma$ , in addition to the term proportional to  $(2J+1)(\Gamma_p/\Gamma)^2$ . Since the latter term is negligible at all angles, according to the present results, only the product  $(2J+1)\Gamma_p/\Gamma$  may be obtained from these scattering data.

Fortunately, the angular distribution of the 4.43-MeV gamma radiation from reaction II at this resonance is consistent only<sup>7,8</sup> with  $J=1^+$  or  $J=2^-$ ; the latter is excluded by the present work. The solid curves of Fig.

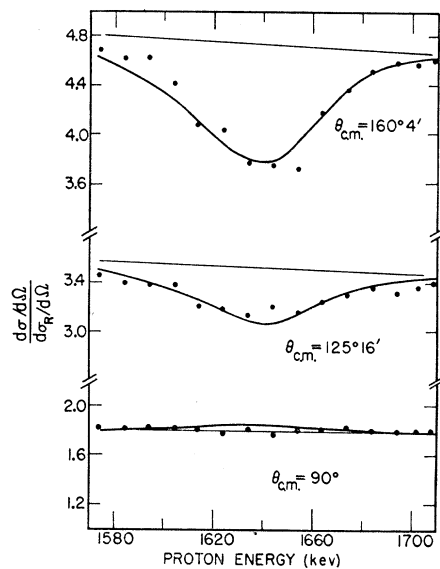


FIG. 10. Excitation functions of the elastic scattering near the 1640-keV resonance. The curves have been calculated for  $E_R=1640$  keV,  $\Gamma=68$  keV,  $\Gamma_p/\Gamma=0.15$ , and  $J=1^+$ .

10 have been calculated for  $J=1^+$ , using the known channel spin ratio  $\alpha=1/14$ . The product  $(2J+1)\Gamma_p/\Gamma=0.45$  was found to give the best agreement between the calculated and observed cross sections, implying that  $\Gamma_p/\Gamma=0.15$ . The reaction cross section calculated from these values is 0.17 barn, to be compared with the measured 0.34 barn.<sup>8</sup> An explanation of this difference has not been found.

$E_p=1210$  keV.—The scattering data near 1210 keV are shown in detail in Fig. 11. The existence of an interference minimum at  $90^\circ$  is inconsistent with formation of this state by any odd value of the incident proton orbital angular momentum and hence excludes an even parity assignment. That reaction I is resonant at 1210 keV implies that the assignment must be even-even or odd-odd. Formation by  $s$ -,  $d$ -, and perhaps  $g$ -wave protons would be possible, but higher values of

the orbital proton momentum would require order-of-magnitude violations of the single-particle limit. The complexity of the observed reaction angular distributions excludes  $s$ -wave formation,<sup>2,5,8</sup> and  $g$ -wave formation would require the interference minimum in the scattering cross section at  $90^\circ$  to occur at an energy greater than the resonance energy. Therefore, only formation by  $d$ -waves is consistent with the scattering data, allowing the assignments  $J=1^-$ ,  $2^-$ , or  $3^-$ . The complexity of the reaction data excludes  $J=1^-$ , and  $J=2^-$  is even-odd. The assignment  $J=3^-$  is consistent with the scattering data, as shown by the solid curves in Fig. 11, which were calculated for  $J=3^-$ ,  $\Gamma_p/\Gamma=0.18$ . The reaction cross section calculated from these values is 0.63 barn, which is in good agreement with the measured 0.68 barn.<sup>5,22</sup>

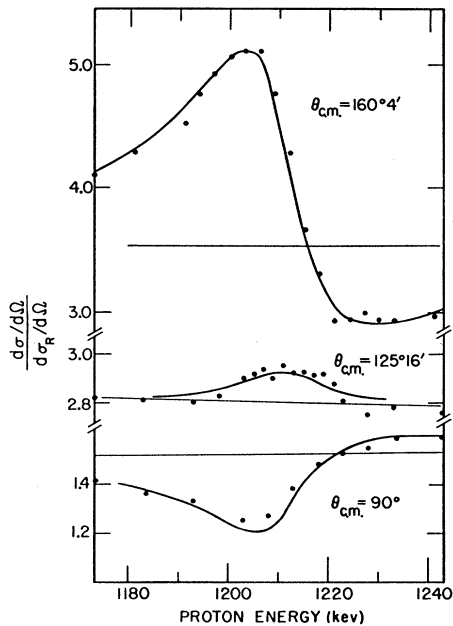


FIG. 11. Excitation functions of the elastic scattering near the 1210-keV resonance. The curves have been calculated for  $E_R=1210$  keV,  $\Gamma=22.5$  keV,  $\Gamma_p/\Gamma=0.18$ , and  $J=3^-$ .

A serious discrepancy arises, however, in that the angular distribution of the  $\alpha$  particles from reaction II, measured by Kraus *et al.*,<sup>5</sup> seems to show that the 1210-keV resonance is formed by  $f$ -wave protons and has  $J=4^+$ . Since the  $N^{15}$  targets used in the present work permitted a measurement of this  $\alpha$ -particle angular distribution over a much larger angular range than was reported previously, the distribution was remeasured. These results are presented in Fig. 12. In this figure, the solid line is a calculated curve for  $d$ -wave proton formation and  $p$ -wave  $\alpha$ -particle decay of a  $J=3^-$  state, while the dashed line is calculated for  $f$ -wave proton formation and  $d$ -wave  $\alpha$ -particle decay of a  $J=4^+$  state. These data are in good agreement with the previous work and are inconsistent with the assignment  $J=3^-$ .

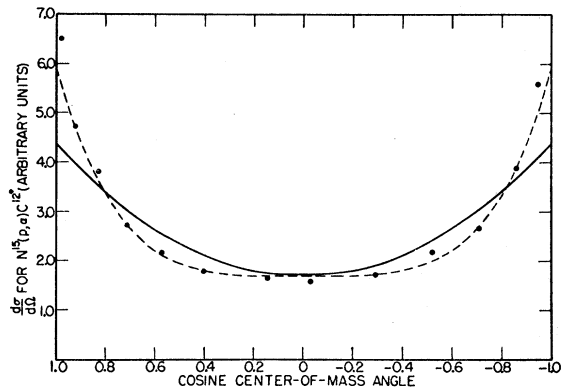


FIG. 12. Angular distribution of the  $\alpha$  particles from reaction II at the 1210-keV resonance. The solid curve has been calculated for  $J=3^-$ ,  $l_p=2$ , and  $l_\alpha=1$ . The dashed curve has been calculated for  $J=4^+$ ,  $l_p=3$ , and  $l_\alpha=2$ .

Two other kinds of measurements at the 1210-keV resonance have also been reported. An angular distribution of the  $\alpha$  particles from reaction I favors  $J=3^-$  but cannot exclude  $J=4^+$  conclusively,<sup>22</sup> and angular distributions<sup>1,5,8</sup> of the 4.43-MeV gamma radiation from reaction II have been shown to be consistent with either  $J=3^-$  or  $4^+$ .

In an effort to clarify the nature of this state, the angular correlation between the  $\alpha$  particles and the gamma radiation from reaction II was measured. The  $\alpha$  particles were detected at a fixed angle with respect to the incident proton beam ( $90^\circ$  in the center-of-mass system), and the angular position of the gamma detector was varied in the plane containing the incident proton beam and the  $\alpha$ -particle detector. The resulting angular correlations are shown in Fig. 13, where the solid curve has been calculated for the  $J=3^-$  case and the dashed curve for  $J=4^+$ . Both curves have been modified to take into account the finite solid angles of the detectors. These results are clearly inconsistent with  $J=4^+$  but are in reasonable agreement with  $J=3^-$ .

An attempt has been made to obtain agreement among these various measurements by calculating angular distributions for a  $J=3^-$  state which is formed by a mixture of  $d$ - and  $g$ -wave protons and which decays (reaction II) by a mixture of  $p$ - and  $f$ -wave  $\alpha$  particles. No single set of mixtures was found which gave satis-

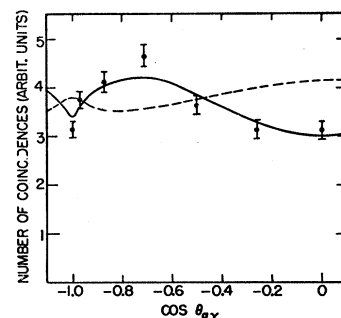


FIG. 13. Angular correlation of the  $\alpha$  particles and 4.43-MeV  $\gamma$  rays from reaction II at the 1210-keV resonance. The solid curve has been calculated for  $J=3^-$ ,  $l_p=2$  and  $l_\alpha=1$ . The dashed curve has been calculated for  $J=4^+$ ,  $l_p=3$ , and  $l_\alpha=2$ . Both curves include the effects of the finite solid angles of the detectors.

factory agreement with the present results and with the 4.43-Mev gamma angular distributions. In this calculation, only the ratios of  $d$ -wave to  $g$ -wave and  $p$ -wave to  $f$ -wave amplitudes were used as fitting parameters; the relevant phase differences were calculated. The  $g$ -wave proton amplitude was shown to be negligible, and the 4.43-Mev gamma distribution and the  $\alpha$ - $\gamma$  correlation were both shown to be consistent with the supposition that the  $f$ -wave partial  $\alpha$ -particle width was about 2.5% of the  $p$ -wave  $\alpha$ -particle width. However, no ratio of these partial widths provides a calculated curve based on the  $J=3^-$  assignment which is consistent with the data of Fig. 12. Moreover, if one arbitrarily allows the phase difference between the  $p$ -wave and  $f$ -wave  $\alpha$  particles to be a fitting parameter in addition to the ratio of the partial widths, satisfactory agreement among the  $\alpha$ -particle angular distributions, the 4.43-Mev gamma angular distribution, and the  $\alpha$ - $\gamma$  angular correlation is still not obtained.

The source of this discrepancy remains obscure. However, while the assignment for the 1210-keV state has not been conclusively established as  $J=3^-$ , there is very strong evidence from both the elastic scattering and the  $\alpha$ - $\gamma$  angular correlation requiring this assignment.

#### IV. DISCUSSION

A comparison of the states in  $O^{16}$  under discussion here with the low-lying states in  $N^{16}$  is of some interest. The first  $T=1$  state in  $O^{16}$  is expected to be near 12.9 Mev.<sup>23</sup> Since this is the region which was investigated in the present work, one might hope that some of these  $O^{16}$  states are the analogs of the first four states in  $N^{16}$ . Warburton and McGruer<sup>24</sup> and Wilkinson<sup>25</sup> have recently shown these  $N^{16}$  states most likely to be  $J=2^-$ ,  $0^-$ ,  $3^-$ , and  $1^-$  respectively. Four states in  $O^{16}$  near 12.9 Mev are indeed observed for which these spin and parity assignments have been reasonably well established. Wilkinson<sup>26</sup> has previously concluded that the  $J=2^-$  state near 898 keV and the  $J=1^-$  state near 1028 keV are very likely the predominantly  $T=1$  states corresponding to the first and fourth states of  $N^{16}$ . By further comparing spins and parities, one is led to suggest that the 710-keV and 1210-keV states are also predominantly  $T=1$  and correspond to the second and third states in  $N^{16}$ .

It is also of interest to compare the reduced neutron widths of the  $N^{16}$  states with the reduced proton widths of the suggested analog states in  $O^{16}$ . Warburton and McGruer<sup>24</sup> have obtained neutron reduced widths by fitting Butler-theory cross section expressions to their

measured  $N^{15}(d,p)N^{16}$  cross sections. However, Tobocman and Kalos<sup>27</sup> have found that the Butler theory is much less reliable for determining reduced widths than for determining the orbital angular momentum of the captured particle. It has been suggested<sup>28</sup> that the extraneous factors responsible for this unreliability are largely eliminated in taking a ratio of two reduced widths if the corresponding two states are formed by the same orbital angular momentum. In  $N^{16}$  the first and third states are formed by  $l=2$  neutrons while the second and fourth states result from the capture of  $l=0$  neutrons. The ratios of the reduced neutron widths are 1.14 and 1.05 for first/third and second/fourth respectively. Corresponding ratios of the proton reduced widths for the  $O^{16}$  analog states obtained from the present work are 1.19 and 1.10. The good agreement between the neutron and proton reduced width ratios lends support to the supposition that the first four predominantly  $T=1$  states in  $O^{16}$  are those near  $E_p=710, 898, 1028,$  and  $1210$  keV. Since the fifth state in  $N^{16}$  is reported to be more than 3 MeV above the first four,<sup>24</sup> all other states in  $O^{16}$  in this region should be predominantly  $T=0$ .

However, it should not be overlooked that the state in  $O^{16}$  which is resonant for 429-keV protons on  $N^{15}$  is also  $J=2^-$  and that the state near 340 keV may be  $J=1^-$ . Appreciable mixing may occur between  $T=0$  and  $T=1$  states of the same spin and parity if the difference in excitation energies is only a few hundred keV, so it may be expected that two of these  $T=1$  states could have significant admixtures of  $T=0$  character. It can moreover be shown that, aside from the fact that the excitation energy is slightly closer to the predicted value, the 898-keV state is not much more likely to be predominantly  $T=1$  than is the 429-keV state. The  $N^{15}(p,\alpha\gamma)C^{12}$  reaction cross section at 429 keV may be obtained from the literature<sup>2,5</sup> and the ratio of the partial proton width to the total width may be expressed as a double-valued function of this reaction cross section. Application of the single-particle limit

TABLE I. Properties<sup>a</sup> of five excited states of  $O^{16}$  reached by  $N^{15}+p$ .

$E_R$ (keV)	$\Gamma$ (keV)	$J\pi$	$l_p$	$\Gamma_p/\Gamma$	$\theta_p^2$	$T$
$710 \pm 7$	$40 \pm 4$	$0^-$	0	1.0	0.11	1
$898 \pm 1^b$	$2.2 \pm 0.2^b$	$2^-$	2	0.56	0.088	1
$1028 \pm 10$	$140 \pm 10$	$1^-$	0	0.8	0.10	1
$1210 \pm 3^b$	$22.5 \pm 1^b$	$3^-$	2	0.18	0.074	1
$1640 \pm 3^c$	$68 \pm 3^c$	$1^+$	1	0.15	0.008	0

<sup>a</sup> In this table, the spin and parity are denoted by  $J\pi$ , the orbital momentum of the captured proton is represented by  $l_p$ ,  $\Gamma_p/\Gamma$  is the ratio of the partial proton width to the total width,  $\theta_p^2$  is the fraction of  $3\beta^2/2MR^2$  which equals the observed partial proton reduced width, and  $T$  is the probable predominant value of the isotopic spin quantum number. An interaction radius of  $4.88 \times 10^{-13}$  cm has been assumed in the calculation of  $\theta_p^2$ .

<sup>b</sup> Reference 2.  
<sup>c</sup> Reference 22.

<sup>27</sup> W. Tobocman and M. H. Kalos, Phys. Rev. **97**, 132 (1955).

<sup>28</sup> T. Auerbach and J. B. French, Phys. Rev. **98**, 1276 (1955).

<sup>23</sup> F. Ajzenberg and T. Lauritsen, Boston University Quarterly Progress Report No. 4, September 30, 1954, (unpublished), Appendix B.

<sup>24</sup> E. K. Warburton and J. N. McGruer, Phys. Rev. **105**, 639 (1957).

<sup>25</sup> D. H. Wilkinson, Phys. Rev. **105**, 686 (1957).

<sup>26</sup> D. H. Wilkinson, Phil. Mag. **1**, 379 (1956).



eliminates one choice, leaving  $\Gamma_p/\Gamma=0.03$ . A reduced width approximately 0.04 of the single-particle limit is implied, and this reduced width compares as favorably with the stripping reduced width as does that for the 898-keV state, in view of the uncertainty of the value of  $\Gamma_p$  for the 429-keV state. Fortunately, the situation is more clearly resolved with respect to the 340-keV state. Since the  $N^{15}(p,\gamma)O^{16}$  cross section is so small near 340 keV,<sup>7</sup> it appears that if the correct assignment is  $J=1^-$  then this gamma transition is inhibited by isotopic spin selection rules, making the 340-keV state predominantly  $T=0$  and the 1028-keV state predominantly  $T=1$ .

Table I is a summary of the available information for the five excited states in  $O^{16}$  studied in the present work. References are given for the values of resonance energies and total widths which were used in the analysis of the scattering data but which were obtained from other work.

#### ACKNOWLEDGMENTS

The author wishes to express his gratitude to Professor T. Lauritsen, Professor W. A. Fowler, Professor C. C. Lauritsen, Professor R. F. Christy, and Dr. F. S. Mozer for assistance, advice, and helpful discussions during the course of this work.

### Study of the $B^{11}+p$ Reactions

G. DEARNALEY, G. A. DISSANAIKE,\* A. P. FRENCH,† AND G. LINDSAY JONES‡

*Cavendish Laboratory, Cambridge, England*

(Received July 15, 1957)

This paper describes a detailed study of the  $B^{11}(p,\alpha_0)Be^8$ ,  $B^{11}(p,\alpha_1)Be^{8*}(2\alpha_2)$ , and  $B^{11}(p,p)$  processes for the region of proton energies spanning the resonances at 0.67 MeV and 1.4 MeV. The measurements include excitation functions and angular distributions, together with the angular correlation between  $\alpha_1$  and  $\alpha_2$  as inferred from the alpha-particle energy spectrum in fixed geometry. The results are analyzed theoretically and are discussed in relation to the findings of other investigators. It is concluded that the complete body of data can be accounted for if the 0.67-MeV resonance (16.57-MeV state of  $C^{12}$ ) is  $(2^-)$  and the 1.4-MeV resonance (17.22-MeV state of  $C^{12}$ ) is  $(1^-)$ , both formed mainly by  $s$ -wave protons; this would corroborate the preferred assignments previously suggested. The proton elastic scattering data imply that the ratio  $\Gamma_p/\Gamma$  is 0.5 for the 0.67-MeV resonance and 0.05 for the 1.4-MeV resonance.

#### I. INTRODUCTION

THE bombardment of boron-11 with protons, one of the first studied of all nuclear reactions, has presented a curiously intractable problem in the matter of its detailed analysis. The main difficulty is the occurrence of several very broad resonances with an extensive overlap, so that the compound state of  $C^{12}$  formed at any given proton energy must normally be thought of as a superposition of states. As a result of this it has been almost impossible to arrive at a clear-cut interpretation of the reaction through studies of only one or two of the possible reaction products. The present paper is the outcome of several investigations (beginning in 1952) carried out with the aim of making our picture of the reaction as complete as possible. None of this work has been previously reported by us, although some of it has been alluded to in papers by other authors.<sup>1-3</sup>

The main concern of this paper is the analysis of the two levels in  $C^{12}$  formed at 0.67 and 1.4 MeV in the proton bombardment of  $B^{11}$ . The present work had its origin in the discovery,<sup>4</sup> at this laboratory, of the now familiar fact that the resonance formed by protons of 0.163 MeV is able to interfere with another level of opposite parity. The earlier measurements were made solely on the long-range alpha particles ( $\alpha_0$ ) leading to the ground state of  $Be^8$ ; to facilitate later discussion we shall enumerate this and all other reactions of interest:

$$B^{11}+p \rightarrow Be^8+\alpha_0, \quad (a)$$

$$\rightarrow Be^{8*}+\alpha_1, \quad (Be^{8*} \rightarrow 2\alpha_2), \quad (b)$$

$$\rightarrow C^{12}+\gamma_0, \quad (c)$$

$$\rightarrow C^{12*}+\gamma_1, \quad (d)$$

$$\rightarrow B^{11}+p. \quad (e)$$

It was soon discovered, from measurements on the energy dependence of the yield of alpha particles<sup>1,5</sup> and

\* Now at the Physical Laboratories, University of Ceylon, Colombo, Ceylon.

† Now at the Physics Department, University of South Carolina, Columbia, South Carolina.

‡ Now at Clifton College, Bristol, England.

<sup>1</sup> Beckman, Huus, and Zupančič, *Phys. Rev.* **91**, 606 (1953).

<sup>2</sup> H. E. Gove and E. B. Paul, *Phys. Rev.* **97**, 104 (1955).

<sup>3</sup> Geer, Nelson, and Wolicki, *Phys. Rev.* **100**, 215 (1955).

<sup>4</sup> Thomson, Cohen, French, and Hutchinson, *Proc. Phys. Soc. (London)* **A65**, 745 (1952).

<sup>5</sup> G. A. Dissanaïke and A. P. French (unpublished).